Earth and Planetary Science Letters 482 (2018) 388–395

Contents lists available at ScienceDirect

Earth and Planetary Science Letters

www.elsevier.com/locate/epsl

Estimating the formation age distribution of continental crust by unmixing zircon ages

Jun Korenaga

Department of Geology and Geophysics, Yale University, P.O. Box 208109, New Haven, CT 06520-8109, USA

ARTICLE INFO

Article history:
Received 5 October 2017
Received in revised form 15 November 2017
Accepted 16 November 2017
Available online xxxx
Editor: A. Yin

Keywords:
continental growth
crustal recycling
plate tectonics

ABSTRACT

Continental crust provides first-order control on Earth's surface environment, enabling the presence of stable dry landmasses surrounded by deep oceans. The evolution of continental crust is important for atmospheric evolution, because continental crust is an essential component of deep carbon cycle and is likely to have played a critical role in the oxygenation of the atmosphere. Geochemical information stored in the mineral zircon, known for its resilience to diagenesis and metamorphism, has been central to ongoing debates on the genesis and evolution of continental crust. However, correction for crustal reworking, which is the most critical step when estimating original formation ages, has been incorrectly formulated, undermining the significance of previous estimates. Here I suggest a simple yet promising approach for reworking correction using the global compilation of zircon data. The present-day distribution of crustal formation age estimated by the new "unmixing" method serves as the lower bound to the true crustal growth, and large deviations from growth models based on mantle depletion imply the important role of crustal recycling through the Earth history.

1. Introduction

At present, continental crust occupies approximately 40% of Earth's surface, and regarding its surface age (Goodwin, 1996), its majority (∼70%) is younger than 1 Ga, and only ∼5% has Archean ages (2.5–4 Ga). Because of crustal reworking such as orogenic overprinting, the original ages of ancient crustal formation are hard to survive, and surface ages are expected to be biased to younger ages. Moreover, continental crust can be recycled to the mantle via erosion and subduction. To understand how continental crust has evolved through time, therefore, we need to delineate the effects of crustal reworking as well as crustal recycling from the geological record. To this end, it is of vital importance to recognize that there are two distinct types of models among a wide variety of 'continental growth' models that have been proposed so far (e.g., Armstrong, 1981; Taylor and McLennan, 1985; Campbell, 2003; Harrison, 2009; Cawood et al., 2013; Iizuka et al., 2017). The first type of models is based on the reconstruction of true crust formation ages by using, for example, K–Ar and Rb–Sr ages (Hurley and Rand, 1969), Nd model ages (DePaolo, 1981; Allegre and Rousseau, 1984), U–Pb ages (Condie, 1998; Rino et al., 2004), or Hf model ages (Belousova et al., 2010; Dhuime et al., 2012; Roberts and Spencer, 2015). All of these models are estimates on the present-day distribution of crust formation ages. Such estimates by themselves contain no information on what has been lost to the mantle by recycling, so these crust-based models serve as the lower bound for net crustal growth. The second type of models is based on the secular evolution of mantle depletion (DePaolo, 1980; Jacobsen, 1988; Armstrong, 1991; Campbell, 2003). As the continental crust is highly enriched in incompatible elements, its extraction from the mantle leaves the residual mantle correspondingly depleted, and crustal recycling can reduce the degree of mantle depletion. From the evolution of mantle depletion, therefore, one can backtrack how the mass of coexisting continental crust should have varied with time. This mantle-based approach provides an estimate on net crustal growth. The effect of crustal reworking is reflected in the difference between crust-based models and the present-day surface age distribution, and that of crustal recycling in the difference between mantle-based and crust-based models. If mantle-based and crust-based models are similar to each other, for example, it would leave little room for crustal recycling.

Crust-based growth models, i.e., efforts to unveil true formation ages based on isotopic signatures preserved in igneous and sedimentary rocks, have steadily been elaborated in the last several decades (Hurley and Rand, 1969; DePaolo, 1981; Allegre and Rousseau, 1984; Condie, 1998; Rino et al., 2004; Kemp et al., 2010), and currently the most popular approach exploits the U–Pb–Hf isotope analyses of detrital zircons (Kemp and Hawkesworth, 2014).

E-mail address: jun.korenaga@yale.edu.

https://doi.org/10.1016/j.epsl.2017.11.039
0012-821X/

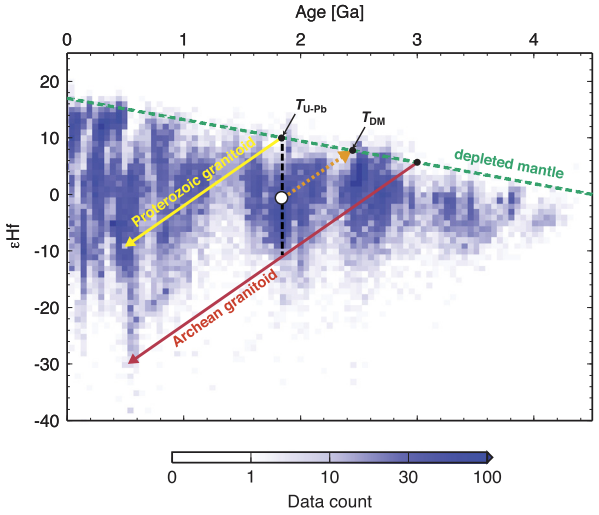

Fig. 1. Distribution of ϵHf and crystallization age data for the global zircon database of Roberts and Spencer (2015). ϵHf is defined as $[(^{176}Hf/^{177}Hf)_{sample}/(^{176}Hf/^{177}Hf)_{CHUR} - 1] \times 10^4$, where CHUR represents chondritic uniform reservoir (Blichert-Toft and Albarede, 1997), calculated at the crystallization age of sample. The evolution of depleted mantle (Vervoort and Blichert-Toft, 1999) is shown as green dashed line. Two kinds of zircon ages, T_{U-Pb} and T_{DM}, are indicated for a hypothetical datum (open circle). A sample mixing scenario for the datum is schematically drawn; an Archean crust evolving along red arrow is reworked by the formation of a Proterozoic crust, which itself evolves along yellow arrow. (For interpretation of the references to color in this figure legend, the reader is referred to the web version of this article.)

Thanks to the peculiar physiochemical properties of zircon, its crystallization age can be determined accurately by U–Pb dating, and it can retain the Hf and oxygen isotopic signatures of its host rock through multiple sedimentary cycles. As detrital zircons sample broad regions of continental upper crust, the global compilations of detrital zircon data have frequently been used to estimate the history of continental growth (Rino et al., 2004; Iizuka et al., 2010; Belousova et al., 2010; Dhuime et al., 2012). Whereas earlier studies are based solely on the distribution of U–Pb crystallization ages (T_{U-Pb}) (Condie, 1998; Rino et al., 2004), more recent studies exploit Hf isotope data to calculate depleted mantle model ages (T_{DM}) (Fig. 1) and correct for the effect of crustal reworking (Belousova et al., 2010; Dhuime et al., 2012). This study presents major improvements on these crust-based models, by providing a new method to properly correct for crustal reworking.

2. Correcting for crustal reworking using zircon data

As crustal reworking can reset crystallization ages, directly using T_{U-Pb} as crust formation ages is expected to be biased to younger ages. Such bias can easily be visualized with the help of synthetic data (Fig. 2a, d, h). It can also be seen that directly using T_{DM} is not appropriate, either, because it is still affected by crustal reworking (Fig. 1). Belousova et al. (2010) proposed to estimate the distribution of crust formation ages by taking the ratio of T_{U-Pb} and T_{DM}, and this approach was also adopted by Dhuime et al. (2012), with a modification to screen out supracrustal zircons using oxygen isotope data. An estimate on the distribution of formation ages by this ratio method is hereinafter referred to as the T_{B-D} distribution. The ratio method is, however, inherently biased to older ages (Fig. 2b, e, i; see also Methods). It appears to work well only when the true formation age is skewed toward older ages (Fig. 2a–c), but this should be viewed as a mere coincidence.

An entirely different approach is possible by noting that crustal reworking can be viewed as mixing between a juvenile magma component derived from the depleted mantle and a reworked crustal component (Kemp et al., 2007; Jagoutz et al., 2009; Iizuka et al., 2010) (Fig. 1). The depleted mantle model age T_{DM} may be modeled as $(1-\alpha)T_1 + \alpha T_2$, where T_1 and T_2 denote the formation ages of the juvenile magma and reworked crustal components, respectively, and α is the reworking index that measures the relative significance of these two components (Iizuka et al., 2010). As T_{U-Pb} is equivalent to T_1, the age of the reworked crustal component can be computed as:

$$T_2 = T_{U-Pb} + \alpha^{-1}(T_{DM} - T_{U-Pb}). \quad (1)$$

Thus, one may undo the mixing by generating two 'pseudodata' with the formation ages of T_1 and T_2 for each pair of T_{U-Pb} and T_{DM}. The ensemble of formation ages generated this way is called hereinafter as T_{unmix}. The reworking index α has been estimated to be approximately 0.5, though it can exhibit both temporal and regional variations (Iizuka et al., 2010). For the simplest application of this "unmixing" method, therefore, α may be set to 0.5; it can also be randomized to propagate the uncertainty of α to T_{unmix} (see Methods). The performance of the unmixing method is also shown in Fig. 2, and for all of the synthetic examples, the distribution of T_{unmix} resembles closely that of true formation ages. One distinct advantage of the unmixing method is to make full use of the joint probability distribution of T_{U-Pb} and T_{DM}, which is equivalent to the two-dimensional (2-D) histogram in the age-ϵHf space (Fig. 1). In contrast, the ratio method projects the 2-D distribution to the 1-D distributions of T_{U-Pb} and T_{DM}, and by doing so, it discards any existing correlation between T_{U-Pb} and T_{DM}.

The unmixing method appears to be statistically robust as well. Fig. 3 presents two additional synthetic tests, the first of which uses data prepared by fully randomizing the reworking index α between 0 and 1. The randomization of this degree can effectively include the uncertainty of T_{DM} originating in the assumed Lu/Hf ratio (Methods). The unmixing procedure is still conducted with $\alpha = 0.5$. Whereas the recovery of the formation age distribution certainly deteriorates to some extent, all of the four peaks in the true distribution are still resolved (Fig. 3c), and the difference caused by random mixing is minor in the cumulative distribution (Fig. 3d). All of synthetic data so far are prepared by single-step mixing, so the good performance of the unmixing method may not be surprising. In the second test, therefore, multi-step mixing is employed to emulate more realistic crustal reworking (Iizuka et al., 2010) (see Methods; Fig. 3e). Interestingly, this additional layer of randomization actually improves the recovery of older formation ages (Fig. 3c). Unmixing multi-step data with the assumption of single-step mixing generally causes a small bias toward older formation ages (Fig. 3f), and this bias helps to compensate the blurring caused by the uncertainty in the reworking index.

Results of yet another synthetic test are given in Fig. 4 to show the performance of the unmixing method when the average of the reworking index α used to prepare synthetic data is different from the value of α assumed by the unmixing method. The most complicated case in the previous synthetic tests (i.e., multi-step mixing with the true formation age distribution of Fig. 2h) is revisited with three different scenarios for the reworking index (Fig. 4a): $\alpha = 0.6 \pm 0.1$, $\alpha = 0.4 \pm 0.1$, and α varying linearly from 0.2 at 4.5 Ga to 0.75 at present. The last case of time-varying α is an attempt to approximate the temporal evolution suggested by Iizuka et al. (2010). The unmixing method is again conducted with $\alpha = 0.5$. As seen in Fig. 4b and 4c, the recovery of the formation age distribution deteriorates to some extent, though the amplitudes of misfit are similar to those seen for the previous tests with different kinds of mixing with the mean α of 0.5 (Fig. 3c and 3d).

3. Application to global zircon data

The unmixing method is applied to a recent global database of detrital zircon (Roberts and Spencer, 2015), which contains

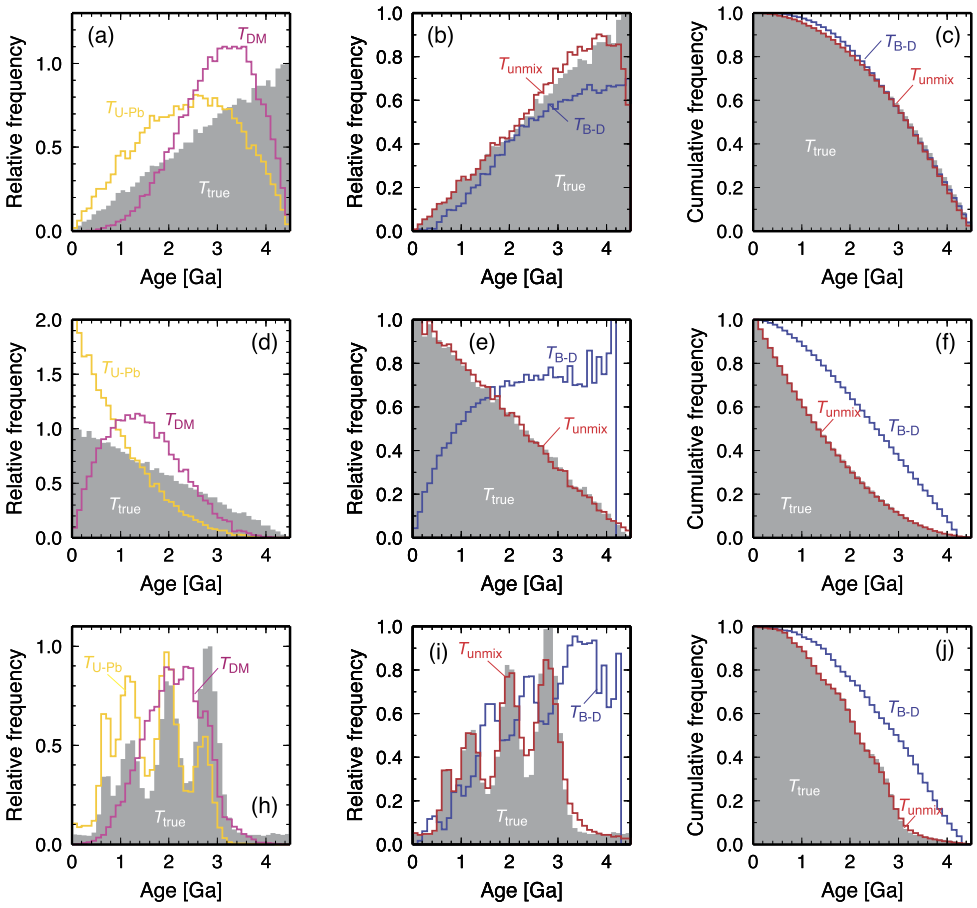

Fig. 2. Recovery test of the ratio method and the unmixing method using three kinds of synthetic data: (a–c) linearly increasing, (d–f) linear decreasing, and (h–j) more complex distributions of crust formation ages. Distribution of true formation ages is shown as gray histogram. Left column shows the distributions of $T_{U\text{–}Pb}$ (yellow) and T_{DM} (magenta) synthesized with single-step mixing, in which α is randomly drawn from the normal distribution with a mean of 0.5 and one standard deviation of 0.1. Middle column compares the distributions of $T_{B\text{-}D}$ (blue) and T_{unmix} (red). Right column shows their cumulative distributions. (For interpretation of the references to color in this figure legend, the reader is referred to the web version of this article.)

~42,000 pairs of $T_{U\text{–}Pb}$ and T_{DM} (Fig. 5). Most of the peaks seen in the $T_{U\text{–}Pb}$ distribution (Fig. 5a) are still recognized in the T_{unmix} distribution, though the background level is increased (Fig. 5b). Those peaks seen in the $T_{U\text{–}Pb}$ distribution correlate well with the supercontinental cycle, and it has long been debated whether they reflect enhanced crustal generation (Condie, 1998) or better preservation potential (Hawkesworth et al., 2010). As such peaks become considerably blurred in the distribution of T_{DM} (Fig. 5a), crustal growth models based simply on T_{DM} could question the significance of supercontinental cycle in the formation of continental crust (Iizuka et al., 2017). In contrast, the T_{unmix} distribution retains those peaks clearly, and the heights of different peaks become comparable after correcting crustal reworking, implying a uniformitarian view for the role of supercontinental formation in crustal evolution. It is important that the T_{unmix} distribution (Fig. 5b) is different from both the $T_{U\text{–}Pb}$ and T_{DM} distributions (Fig. 5a). If the $T_{U\text{–}Pb}$ distribution is directly used as the true formation ages (Condie, 1998; Condie and Aster, 2010), it would give an impression that most of extant crust has formed after 3 Ga. If the T_{DM} distribution is used instead, the formation ages would be skewed toward the middle of the Earth history. The T_{unmix} distribution suggests that the generation of (extant) crust is already nontrivial at the beginning of the Earth history and gradually increases until ~3 Ga, after which it maintains a nearly steady level, with occasional elevations caused by supercontinental formation.

As the method processes individual data one by one, it is straightforward to incorporate various data-specific operations (see Methods). As an example, results with the oxygen isotope screening as parameterized by Dhuime et al. (2012) are also shown for comparison. In terms of the cumulative distribution, the effect of oxygen isotope screening is minimal (Fig. 5c), which is reassuring because how to use oxygen isotopes for screening is still debated (Roberts and Spencer, 2015). The T_{unmix} distribution is very different from the earlier estimates based on similar global compilations of zircon data (Belousova et al., 2010; Dhuime et al., 2012) (Fig. 5c), and this is owing to the inherent bias caused by the ratio method employed in those studies (Fig. 2; Methods).

The cumulative T_{unmix} distribution is an estimate on the present-day cumulative distribution of crust formation age, which should be seen as the lower bound for the net crustal growth. For example, about 40% of the present-day crust is estimated to have formation ages greater than 2.5 Ga (Fig. 5c), so at least this fraction of the present-day crustal mass should have existed at 2.5 Ga. The actual crustal mass at 2.5 Ga could have been higher, and in this case, any excess from the presently preserved crust must have been recycled back to the mantle. Zircon age data allow us to correct for crustal reworking, but not for crustal recycling.

The T_{unmix} distribution is a lower bound in another sense as well. A prevailing assumption in zircon-based studies is that individual zircon samples represent different crustal volumes of similar sizes. Zircon saturation, however, depends on the temperature and composition of parental magma (Watson and Harrison, 1983; Boehnke et al., 2013), and higher mantle potential temperatures early in the Earth history (Herzberg et al., 2010), for example,

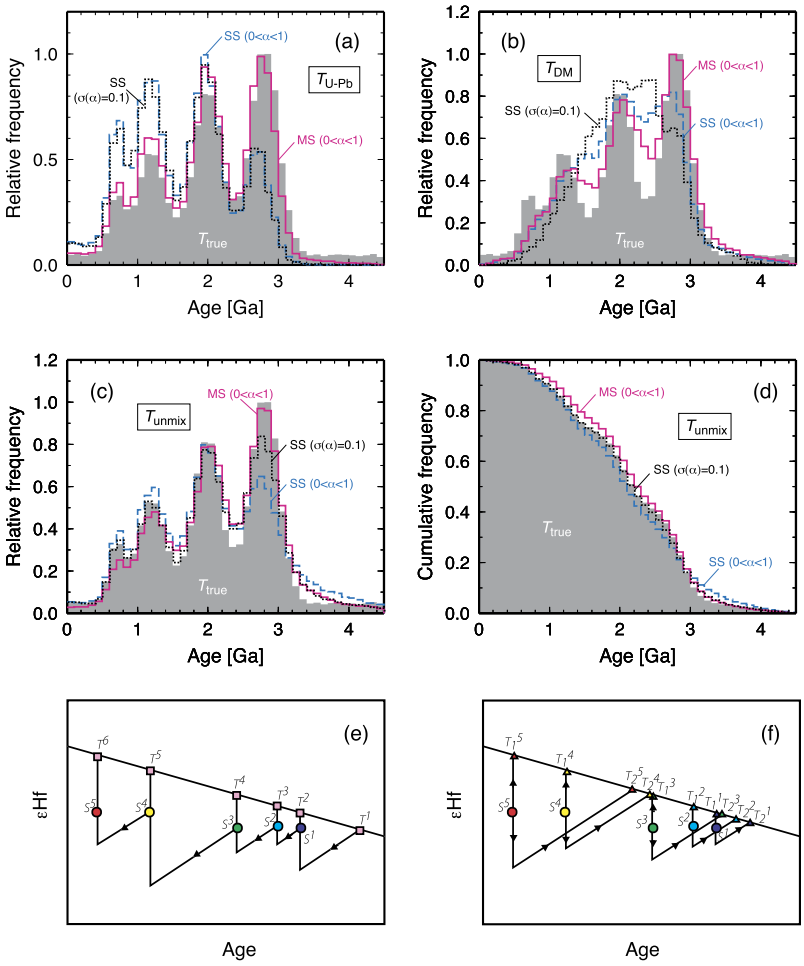

Fig. 3. Further recovery test of the unmixing method with more extensively randomized synthetic data. Distributions of (a) synthesized $T_{U\text{–}Pb}$, (b) synthesized T_{DM}, and (c) T_{unmix} are compared with that of true formation ages (gray histogram). (d) is same as (c) but for cumulative distribution. (e) Schematic drawing for multi-step mixing, and (f) that for corresponding single-step unmixing procedure (T^i, S^i, and $T^i_{1,2}$ denote true formation ages, synthetic zircon data, and pseudodata, respectively). See Methods for the detail of synthetic data preparation. For all cases, the unmixing method is conducted with $\alpha = 0.5$.

may have resulted in magmas depleted in zircon relative to the present (Keller et al., 2017). In other words, older zircon samples could represent greater crustal volumes. Treating all zircon samples equally thus minimizes the estimate on crustal volume preserved from the early Earth. Similar caution also exists for regional variations among zircon samples with similar ages; a single pluton with high Zr concentration could make many more zircons per mass of generated continental crust. The use of a global compilation could minimize the effect of such regional variations, but as mentioned earlier, the unmixing method itself can easily incorporate data-specific operations, so it is possible to improve the recovery of the true formation age distribution by taking into account the likely nature of source regions. When doing so, it would also be important to better constrain the history of crustal reworking; an incorrect assumption for the mean α leads to a nontrivial estimation error (Fig. 4), but this type of error can be reduced by using proper values of α in unmixing. Such a more careful treatment of existing zircon data undoubtedly requires more information than contained in the literature, so it is not attempted here. The simplicity of the unmixing method, however, will allow us to keep improving the estimate of the crustal formation age distribution by assimilating relevant geological and geochemical data as they become available.

4. Implications for early Earth dynamics and environment

The significance of the new estimate on the present-day distribution of crust formation ages becomes more evident when compared with mantle-based models of net crustal growth (Fig. 5c). Since first proposed in 2010, the application of the ratio method to different compilations of zircon data has yielded similar 'growth' curves (Belousova et al., 2010; Dhuime et al., 2012; Roberts and Spencer, 2015), and owing to this apparent consistency, the standing of these models is quite solid in the recent literature (e.g., Iizuka et al., 2017; Hawkesworth et al., 2017). Such models are also similar to the mantle-based model of Campbell (2003), so different approaches seem to be converging. Being solely based on zircon age data, however, these 'growth' models based on the ratio method can only be an estimate on the present-day distribution of crust formation ages, not net growth models. Whereas the possibility of large-scale crustal recycling has long been discussed (e.g., Allegre and Rousseau, 1984; Gurnis and Davies, 1986), therefore, the apparent convergence of the crust-based model of Dhuime et al. (2012) and the mantle-based model of Campbell (2003) would indicate that crustal recycling had been insignificant through time (Fig. 5c). This inference would be valid if the ratio method could accurately correct for crustal reworking, but as seen in Fig. 2, the method suffers from a strong bias toward older ages, and this bias

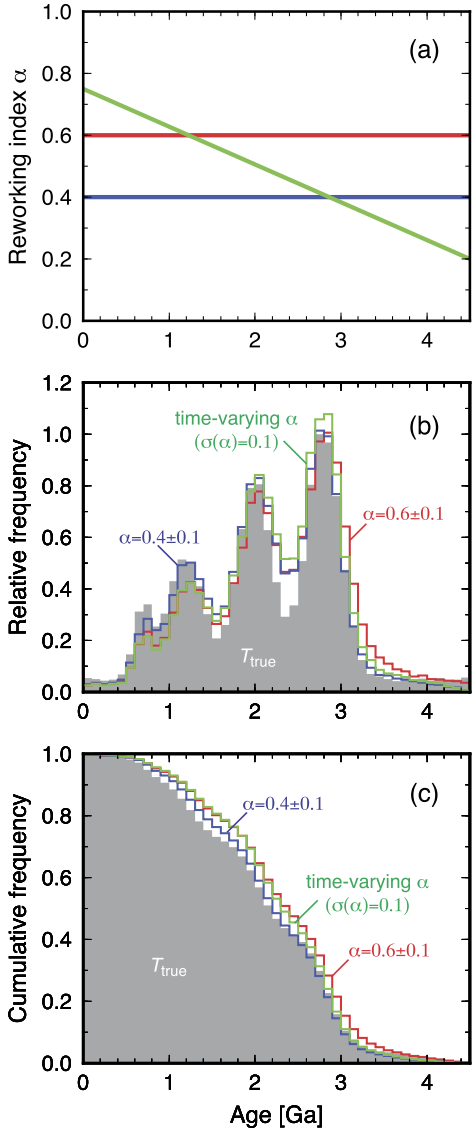

Fig. 4. Effects of bias in the reworking index on the performance of the unmixing method. Synthetic data are prepared with multi-step mixing as done for the case shown in Fig. 3, but with using the reworking index, the average of which is different from 0.5. (a) Three different scenarios used for synthetic data generation: mean α is set to 0.6 (red) or 0.4 (blue), or it is varied linearly from 0.2 at 4.5 Ga to 0.75 at present (green). In all cases, the standard deviation is set to 0.1. (b) Distributions of T_{unmix} are compared with that of true formation ages (gray histogram). (c) is same as (b) but for cumulative distribution. For all cases, the unmixing method is conducted with $\alpha = 0.5$. (For interpretation of the references to color in this figure legend, the reader is referred to the web version of this article.)

is the primary source of the apparent consistency among its previous applications.

With a more likely present-day distribution of crust formation ages such as that given by the T_{unmix} distribution, crustal recycling becomes a significant component of crustal evolution (Fig. 5c, blue arrows). As noted earlier, the T_{unmix} distribution does not take into account the possible evolution of crustal composition, but the mantle-based growth models also usually assume that the continental crust was as similarly enriched in the past as in the present. Thus, the difference between a net growth curve and the cumulative distribution of preserved crust would persist even if we consider the secular change of crustal composition, because both of them will be shifted upward in a similar manner.

Mantle-based models are typically characterized by rapid crustal growth in the early Earth followed by more gradual growth (Fig. 5c). Whereas net crustal growth is slow in this second stage and could even be negligible in the end-member model of Armstrong (1981), the rate of new crust generation should be higher than that of net crustal growth in the presence of crustal recycling. Thus, the new estimate on the present-day distribution of crust formation ages, which points to substantial crustal recycling through time, also suggests the production of new continental crust at a much higher level than indicated by net crustal growth. The evolution of continental crust since the early Archean could potentially be considerably more dynamic than implied by the seemingly slow net growth, being characterized by intensive crustal production and destruction. Such dynamic crustal evolution has important implications for the long-term CO_2 cycle (Kasting and Catling, 2003; Berner, 2004), the oxygenation of the atmosphere (Lyons et al., 2014), and the global water cycle (Korenaga et al., 2017), and resolving its details is essential to better understand the coevolution of the Earth's interior and the surface environment. In this regard, it will be important to evaluate the robustness of mantle-based growth models. For example, the model of Campbell (2003) is based on the secular evolution of Nb/U of the mantle back to the early Archean, but the original Nb/U data, if their scatters are taken into account, do not demand notable crustal growth for the last 3.5 Gyr, being compatible with the model of Armstrong (1981) (note that the original Armstrong model is of conceptual nature but has been argued to be consistent with the evolution of mantle depletion (Armstrong, 1991)). If the true crustal growth is close to the Armstrong model, then, the T_{unmix} distribution may necessitate efficient crustal recycling and thus significant crustal production in the early Earth. Also, it should be noted that the difference between crust-based models and mantle-based ones does not directly reflect the extent of crustal recycling at any given time, but rather the time-integrated effect of crustal recycling. Quantifying the magnitude of crustal recycling in the past thus requires us to consider crust–mantle evolution as a whole. The present-day distribution of crust formation age, as estimated in this study, will serve as a robust global constraint on the coupled crust–mantle evolution, an improved understanding of which will be indispensable to decipher the initiation of plate tectonics on the Earth (Korenaga, 2013).

5. Methods

5.1. Preparation of synthetic data

Each of the three synthetic tests shown in Fig. 2 is prepared by generating synthetic zircon age data in the following way. First, M different ages are generated with a given relative frequency, $\rho(\tau)$, using the rejection sampling (von Neumann, 1951). These data represent true crust formation ages and are denoted as T^i_{true} ($i = 1, 2, \ldots, M$). Then, the following binary mixing is repeated for $i = 1, 2, \ldots, M$ to prepare M synthetic pairs of $T_{\mathrm{U\text{–}Pb}}$ and T_{DM}: (1) select two integers, k and l, randomly from $[1, M]$, (2) call the younger and older ages of T^k_{true} and T^l_{true} as T_{min} and T_{max}, respectively, (3) set $T^i_{\mathrm{U\text{–}Pb}} = T_{\mathrm{min}}$, and (4) set $T^i_{\mathrm{DM}} = (1-\alpha)T_{\mathrm{min}} + \alpha T_{\mathrm{max}}$, where α is drawn from the normal distribution with a mean of 0.5 and one standard deviation of 0.1. This synthetic data generation is the same as that adopted by Belousova et al. (2010) except that the reworking index α is randomized here. The number of data M is set to 40,000 for all of the examples in this study, and the following three distributions are used for $\rho(\tau)$: (1) $\rho_1(\tau) = \tau/\tau_{\mathrm{max}}$ (Fig. 2a), (2) $\rho_2(\tau) = 1 - \tau/\tau_{\mathrm{max}}$ (Fig. 2b), and (3) $\rho_3(\tau) = a_0 + \sum_{m=1}^{4} a_m \exp[-(\tau - \tau_m)^2/(2\sigma_m^2)]$ (Fig. 2c), where $\tau_{\mathrm{max}} = 4.5$ Ga, $a_0 = 0.05$, $a_1 = 0.3$, $a_2 = 0.5$, $a_3 = 0.8$, $a_4 = 1.0$, $\tau_1 = 0.7$ Ga, $\tau_2 = 1.2$ Ga, $\tau_3 = 2.0$ Ga, $\tau_4 = 2.8$ Ga, $\sigma_1 = 0.1$ Gyr, and $\sigma_2 = \sigma_3 = \sigma_4 = 0.2$ Gyr.

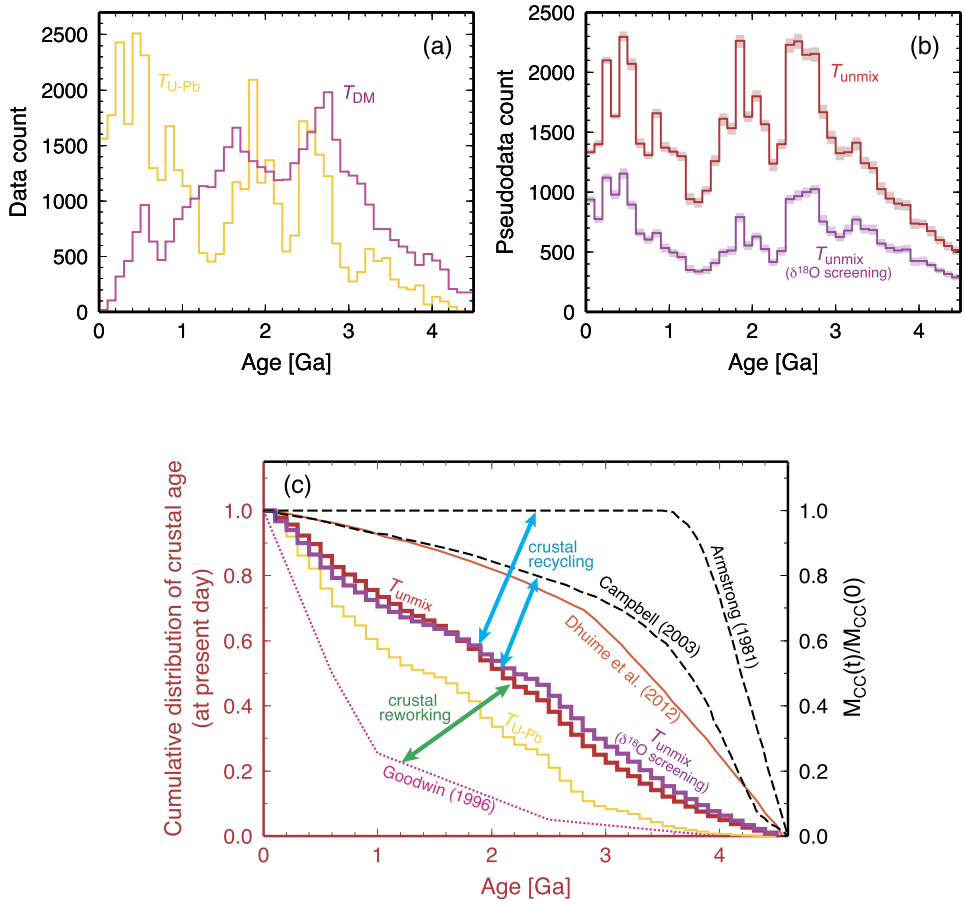

Fig. 5. Application to the global database of Roberts and Spencer (2015). (a) $T_{U\text{–}Pb}$ (yellow) and T_{DM} (magenta). (b) T_{unmix} without (red) and with (purple) oxygen isotope screening. Both α and T_{DM} are randomized during unmixing (see Methods), and shading denotes 90% confidence limit based on 100 iterations. (c) Present-day cumulative distributions of crustal age (warm colors) and net crustal growth models (black dashed), both normalized by the present-day crustal volume (or mass). The former include surface age (Goodwin, 1996) (dotted pink), $T_{U\text{–}Pb}$ (yellow), T_{unmix} (red and purple), and the model of Dhuime et al. (2012) (orange). The latter include the models of Armstrong (1981) and Campbell (2003). (For interpretation of the references to color in this figure legend, the reader is referred to the web version of this article.)

For the first test shown in Fig. 3, the above single-step mixing procedure is used with the distribution $\rho_3(\tau)$, and the reworking index α is drawn from the uniform distribution on the interval $(0, 1)$. For the second test shown in Fig. 3, the following multi-step mixing procedure is repeated until the number of synthetic data reaches M. First, an integer, S, is drawn randomly from a power-law distribution with the range of $[1, S_{max}]$ and the exponent of β, where S_{max} is the maximum number of mixing. Next, select $S+1$ integers, k_j $(j = 1, 2, \ldots, S+1)$, randomly from $[1, M]$, and sort the ages $T^{k_j}_{true}$ in the descending order. Then, iterate the following steps for $j = 2, 3, \ldots, S+1$: (1) set $T_{U\text{–}Pb} = T^{k_j}_{true}$, (2) if j is 2, set $T_{pre} = T^{k_1}_{true}$; otherwise, set T_{pre} to T_{DM} in the previous step, and (3) set $T_{DM} = (1-\alpha)T^{k_j}_{true} + \alpha T_{pre}$, where α is drawn from the uniform distribution on the interval $(0, 1)$. From S-step mixing, S pairs of $T_{U\text{–}Pb}$ and T_{DM} are generated, in which the j-th pair is the result of j-step mixing (Fig. 3e). The maximum number of mixing S_{max} is set to 40, and the exponent β is set to $-3/2$ so that the likelihood of S-step mixing decreases with increasing S. Out of $M = 40{,}000$ synthesized pairs, ~14% is from single-step mixing, ~39% is from 2- to 5-step mixing, ~20% is from 6- to 10-step mixing, and ~28% is from more than 10-step mixing.

To summarize, three kinds of mixing are shown in Fig. 3: (1) single-step (SS) mixing with α drawn from the normal distribution with a mean of 0.5 and one standard deviation of 0.1 (black dotted line); this is what is used for Fig. 2 and is shown for comparison, (2) single-step mixing with α drawn from the uniform distribution on the interval $(0, 1)$ (blue dashed line), and (3) multi-step (MS) mixing with α drawn from the uniform distribution on $(0, 1)$ (red line).

For synthetic tests shown in Fig. 4, the above multi-step mixing with the distribution $\rho_3(\tau)$ is repeated with the following three different scenarios for α: mean α is set to 0.6 (red) or 0.4 (blue), or it is varied linearly from 0.2 at 4.5 Ga to 0.75 at present. In all cases, the standard deviation is set to 0.1.

5.2. The ratio method

Belousova et al. (2010) proposed to estimate the distribution of crust formation age as

$$X(\tau) = \frac{N_{DM}(\tau)}{N_{U\text{–}Pb}(\tau) + N_{DM}(\tau)}, \tag{2}$$

where τ is age, and $N_{U\text{–}Pb}(\tau)$ and $N_{DM}(\tau)$ denote the distributions of $T_{U\text{–}Pb}$ and T_{DM}, respectively, for samples with $T_{DM} \geq T_{U\text{–}Pb}$ (i.e., samples plotted below the depleted mantle evolution line in Fig. 1). This approach was also adopted by Dhuime et al. (2012), with a modification to screen out supracrustal zircons using oxygen isotope data. When calculating Hf model ages, it is common to use $^{176}Lu/^{177}Hf$ of average continental crust (= 0.015) (Griffin et al., 2004), instead of the measured $^{176}Lu/^{177}Hf$ of zircon (usually below 0.005), and such model ages are sometimes referred to as "crustal" model ages (Belousova et al., 2010). How to calculate Hf model ages is the subject of ongoing debates (Roberts and Spencer, 2015); for example, a higher value of

$^{176}Lu/^{177}Hf$ (0.022) is consistent with mafic lithologies (Pietranik et al., 2008). As a possibly neutral choice, the average crustal value ($^{176}Lu/^{177}Hf = 0.015$) is adopted in this study for the calculation of T_{DM}, and T_{DM} in equations (1) and (2) corresponds to crustal model ages as in previous studies (Belousova et al., 2010; Dhuime et al., 2012). In the main text, $X(\tau)$ is referred to as the distribution of $T_{B\text{-}D}$.

In previous studies, the above $X(\tau)$ was integrated to obtain a crustal growth curve, as if $X(\tau)$ were proportional to the generation rate of new crust at age τ, but it cannot be so. As the ratio of two different distributions, the quantity $X(\tau)$ could possibly represent the new crust generation 'ratio', which should be distinguished from the new crust generation 'rate'. It is unclear whether $X(\tau)$ could even be the new crust generation ratio. The performance of the ratio method against three synthetic data can be seen in Fig. 2.

Note that Belousova et al. (2010) also conducted two synthetic tests, the one with the uniform distribution of T_{true} and the other similar to Fig. 2a. Though the ratio method clearly failed the former, the apparent success from the latter was taken as the validation of the method. Belousova et al. (2010) also compared their crustal growth curve to the results of an independent study known as GLAM (Global Lithospheric Architecture Mapping; Begg et al., 2009), which is based on surface geology, seismic tomography, and mantle xenoliths, but this comparison is not very meaningful. First of all, Begg et al. (2009) is not a global model; it is exclusively about the African lithosphere. In addition, seismic tomography does not carry any geochronological information, and petrological sampling by mantle xenoliths is highly sporadic and spatially limited. Finally, continental lithosphere includes continental crust as well as lithospheric mantle (and is dominated by the latter), and it is not directly comparable with continental crust alone.

5.3. The unmixing method

The simplest unmixing operation with $\alpha = 0.5$ is as follows. Let M be the total number of zircon age pairs $T_{U\text{–}Pb}$ and T_{DM}, each of which satisfies $T_{DM} \geq T_{U\text{–}Pb}$. From each pair, create two pseudodata $T_1 = T_{U\text{–}Pb}$, and $T_2 = 2T_{DM} - T_{U\text{–}Pb}$. The distribution of $2M$ pseudodata constitutes directly an estimate on that of crust formation ages. This is what is used for Figs. 2–4.

Because the unmixing method acts on individual data one by one, it is straightforward to incorporate additional data-specific considerations. For example, if a certain subset of zircon data is believed to represent a greater source area than indicated by the number of its data count, one can populate more than two pseudodata from one age pair to properly affect the distribution of formation ages. For the sake of simplicity, all data are treated equally in this study.

To estimate the influence of the uncertainty in the reworking index, T_2 may be calculated using eq. (1) with α drawn from the uniform distribution on the interval $(0, 1)$. Moreover, the depleted mantle model age in the database of Roberts and Spencer (2015) is based on $^{176}Lu/^{177}Hf$ of 0.015 (an average upper crustal value), but one can assess the impact of this assumed value by recalculating T_{DM} with $^{176}Lu/^{177}Hf$ randomly taken from the interval $(0.003, 0.021)$, which covers from an average zircon value to a typical mafic lithology value (Roberts and Spencer, 2015). The unmixing operation for Fig. 5 is conducted with both of the above randomizations. When a randomly drawn α is very small, it could cause T_2 to exceed the age of the Earth, and no pseudodata is produced in such a case.

The database of Roberts and Spencer (2015) does not contain oxygen isotope information, but Dhuime et al. (2012) parameterized $\delta^{18}O$-based screening as a function of the depleted mantle model age, and it can be implemented in the unmixing method as follows. For each data, first calculate the acceptance probability p_a as $p_a = 0.73$ if $T_{DM} > 3.2$ Ga, and $p_a = aT_{DM}^2 + bT_{DM} + c$ otherwise, where $a = 2.894 \times 10^{-7}$, $b = -1.085 \times 10^{-3}$, and $c = 1.243$. Then pick a random number, r, from the interval $(0, 1)$, and if $r > p_a$, do not produce any pseudodata from this data.

Acknowledgements

This material is based upon work supported by the U.S. National Aeronautics and Space Administration through the NASA Astrobiology Institute under Cooperative Agreement No. NNA15BB03A issued through the Science Mission Directorate. The author thanks Mark Harrison and Patrick Boehnke for constructive comments.

References

Allegre, C.J., Rousseau, D., 1984. The growth of the continent through geological time studied by Nd isotope analysis of shales. Earth Planet. Sci. Lett. 67, 19–34.
Armstrong, R.L., 1981. Radiogenic isotopes: the case for crustal recycling on a near-steady-state no-continental-growth Earth. Philos. Trans. R. Soc. Lond. A 301, 443–472.
Armstrong, R.L., 1991. The persistent myth of crustal growth. Aust. J. Earth Sci. 38, 613–630.
Begg, G.C., Griffin, W.L., Natapov, L.M., O'Reilly, S.Y., Grand, S.P., O'Neill, C.J., Hronsky, J.M.A., Poudjom Djomani, Y., Swain, C.J., Deen, T., Bowden, P., 2009. The lithospheric architecture of Africa: seismic tomography, mantle petrology, and tectonic evolution. Geosphere 5, 23–50.
Belousova, E.A., Kostitsyn, Y.A., Griffin, W.L., Begg, G.C., O'Reilly, S.Y., Pearson, N.J., 2010. The growth of the continental crust: constraints from zircon Hf-isotope data. Lithos 119, 457–466.
Berner, R.A., 2004. The Phanerozoic Carbon Cycle: CO_2 and O_2. Oxford Univ. Press.
Blichert-Toft, J., Albarede, F., 1997. The Lu–Hf isotope geochemistry of chondrites and the evolution of the mantle–crust system. Earth Planet. Sci. Lett. 148, 243–258.
Boehnke, P., Watson, E.B., Trail, D., Harrison, T.M., Schmitt, A.K., 2013. Zircon saturation re-revisited. Chem. Geol. 351, 324–334.
Campbell, I.H., 2003. Constraints on continental growth models from Nb/U ratios in the 3.5 Ga Barberton and other Archaean basalt–komatiite suites. Am. J. Sci. 303, 319–351.
Cawood, P.A., Hawkesworth, C.J., Dhuime, B., 2013. The continental record and the generation of continental crust. Geol. Soc. Am. Bull. 125, 14–32.
Condie, K.C., 1998. Episodic continental growth and supercontinents: a mantle avalanche connection? Earth Planet. Sci. Lett. 163, 97–108.
Condie, K.C., Aster, R.C., 2010. Episodic zircon age spectra of orogenic granitoids: the supercontinent connection and continental growth. Precambrian Res. 180, 227–236.
DePaolo, D.J., 1980. Crustal growth and mantle evolution: inferences from models of element transport and Nd and Sr isotopes. Geochim. Cosmochim. Acta 44, 1185–1196.
DePaolo, D.J., 1981. Neodymium isotopes in the Colorado Front Range and crust–mantle evolution in the Proterozoic. Nature 291, 193–196.
Dhuime, B., Hawkesworth, C.J., Cawood, P.A., Storey, C.D., 2012. A change in the geodynamics of continental growth 3 billion years ago. Science 335, 1334–1336.
Goodwin, A.M., 1996. Principles of Precambrian Geology. Academic Press, London.
Griffin, W.L., Belousova, E.A., Shee, S.R., Pearson, N.J., O'Reilly, S.Y., 2004. Archean crustal evolution in the northern Yilgarn Craton: U–Pb and Hf-isotope evidence from detrital zircons. Precambrian Res. 131, 231–282.
Gurnis, M., Davies, G.F., 1986. Apparent episodic crustal growth arising from a smoothly evolving mantle. Geology 14, 396–399.
Harrison, T.M., 2009. The Hadean crust: evidence from >4 Ga zircons. Annu. Rev. Earth Planet. Sci. 37, 479–505.
Hawkesworth, C.J., Cawood, P.A., Dhuime, B., Kemp, A.I.S., 2017. Earth's continental lithosphere through time. Annu. Rev. Earth Planet. Sci. 45, 169–198.
Hawkesworth, C.J., Dhuime, B., Pietranik, A.B., Cawood, P.A., Kemp, A.I.S., Storey, C.D., 2010. The generation and evolution of the continental crust. J. Geol. Soc. Lond. 167, 229–248.
Herzberg, C., Condie, K., Korenaga, J., 2010. Thermal evolution of the Earth and its petrological expression. Earth Planet. Sci. Lett. 292, 79–88.
Hurley, P.M., Rand, J.R., 1969. Pre-drift continental nuclei. Science 164, 1229–1242.
Iizuka, T., Komiya, T., Rino, S., Maruyama, S., Hirata, T., 2010. Detrital zircon evidence for Hf isotopic evolution of granitoid crust and continental growth. Geochim. Cosmochim. Acta 74, 2450–2472.
Iizuka, T., Yamaguchi, T., Itano, K., Hibiya, Y., Suzuki, K., 2017. What Hf isotopes in zircon tell us about crust–mantle evolution. Lithos 274–275, 304–327.
Jacobsen, S.B., 1988. Isotopic and chemical constraints on mantle–crust evolution. Geochim. Cosmochim. Acta 52, 1341–1350.

Jagoutz, O.E., Burg, J.-P., Hussain, S., Dawood, H., Pettke, T., Iizuka, T., Maruyama, S., 2009. Construction of the granitoid crust of an island arc part I: geochronological and geochemical constraints from the plutonic Kohistan (NW Pakistan). Contrib. Mineral. Petrol. 158, 739–755.

Kasting, J.F., Catling, D., 2003. Evolution of a habitable planet. Annu. Rev. Astron. Astrophys. 41, 429–463.

Keller, C.B., Boehnke, P., Schoene, B., 2017. Temporal variation in relative zircon abundance throughout Earth history. Geochem. Perspect. Lett. 3, 179–189.

Kemp, A.I.S., Hawkesworth, C.J., 2014. Growth and differentiation of the continental crust from isotope studies of accessory minerals. In: Treatise on Geochemistry, vol. 4, 2nd ed. Elsevier, pp. 379–421.

Kemp, A.I.S., Hawkesworth, C.J., Foster, G.L., Paterson, B.A., Woodhead, J.D., Hergt, J.M., Gray, C.M., Whitehouse, M.J., 2007. Magmatic and crustal differentiation history of granitic rocks from Hf–O isotopes in zircon. Science 315, 980–983.

Kemp, A.I.S., Wilde, S.A., Hawkesworth, C.J., Coath, C.D., Nemchin, A., Pidgeon, R.T., Vervoort, J.D., DuFrane, S.A., 2010. Hadean crustal evolution revisited: new constraints from Pb–Hf isotope systematics of the Jack Hills zircons. Earth Planet. Sci. Lett. 296, 45–56.

Korenaga, J., 2013. Initiation and evolution of plate tectonics on Earth: theories and observations. Annu. Rev. Earth Planet. Sci. 41, 117–151.

Korenaga, J., Planavsky, N.J., Evans, D.A.D., 2017. Global water cycle and the coevolution of Earth's interior and surface environment. Philos. Trans. R. Soc. Lond. A 375, 20150393. https://doi.org/10.1098/rsta.2015.0393.

Lyons, T.W., Reinhard, C.T., Planavsky, N.J., 2014. The rise of oxygen in Earth's early ocean and atmosphere. Nature 506, 307–315.

Pietranik, A.B., Hawkesworth, C.J., Storey, C.D., Kemp, A.I.S., Sircombe, K.N., Whitehouse, M.J., Bleeker, W., 2008. Episodic, mafic crust formation from 4.5 to 2.8 Ga: new evidence from detrital zircons, Slave craton, Canada. Geology 36, 875–878.

Rino, S., Komiya, T., Windley, B.F., Katayama, I., Motoki, A., Hirata, T., 2004. Major episodic increases of continental crustal growth determined from zircon ages of river sands; implications for mantle overturns in the Early Precambrian. Phys. Earth Planet. Inter. 146, 369–394.

Roberts, N.M.W., Spencer, C.J., 2015. The zircon archive of continent formation through time. In: Roberts, N.M.W., Van Kranendonk, M., Parman, S., Shirey, S., Clift, P.D. (Eds.), Continent Formation Through Time. In: Geol. Soc. (Lond.) Spec. Publ., vol. 389. Geological Society of London, pp. 197–225.

Taylor, S.R., McLennan, S.M., 1985. The Continental Crust: Its Composition and Evolution. Blackwell, Boston.

Vervoort, J.D., Blichert-Toft, J., 1999. Evolution of the depleted mantle: Hf isotope evidence from juvenile rocks through time. Geochim. Cosmochim. Acta 63, 533–556.

von Neumann, J., 1951. Various techniques used in connection with random digits. Natl. Bur. Stand., Appl. Math. Ser. 12, 36–38.

Watson, E.B., Harrison, T.M., 1983. Zircon saturation revisited: temperature and composition effects in a variety of crustal magma types. Earth Planet. Sci. Lett. 64, 295–304.